Generalizations of the Bruggeman equation and a concept of shape-distributed particle composites

Anatoliy V. Goncharenko*
Center for Superfunctional Materials, Department of Chemistry, Pohang University of Science and Technology, Pohang 790-784, Korea
(Received 21 May 2003; published 27 October 2003)

We consider generalizations of the classical symmetrical Bruggeman equation based on the concept of shape-distributed particle systems. The use of the Beta distribution for the particle shape is shown to result in some known as well as unknown equations of the effective medium theory. However, these equations yield no percolation threshold. On the other hand, the use of one- and two-dimensional steplike distributions of spheroidal (ellipsoidal) shapes yields a percolation threshold depending on the distribution parameters. The problem of finding the percolation threshold to fit the systems under consideration, as well as the applicability area of the generalized Bruggeman equation and its relation to the Bergman representation, are discussed.

DOI: 10.1103/PhysRevE.68.041108 PACS number(s): 05.60.Cd, 72.80.Tm, 78.20.Bh

I. INTRODUCTION

Since 1935, when the classical (symmetrical) Bruggeman equation (BE) was put forward [1] up to the present it has been extensively used in various areas of solid state and soft matter physics despite the availability of a rich variety of alternative, more modern homogenization theories. There are numerous examples of using the BE in completely different situations for various effective transport coefficients, such as electric and thermal conductivity, permittivity, permeability, diffusivity, etc. (see, e.g., [2–39]). The Bruggeman theory has also been extended to the somewhat more complex problem of the elastic constants of composite materials [6,40–42]. It should be noted, however, that its use does not always seem justified. Nevertheless, unfortunately very often authors apply the BE to various systems without sufficient reason [43].

What is the reason for this popularity of the BE? Of course, simplicity and the clear physical meaning of the Bruggeman equation play an important role. However, in our view, another fact is also important, namely, for many inhomogeneous systems, for natural and also for artificially prepared composites, the *real values of transport coefficients are close to those predicted by the equation*. This is particularly inherent in systems whose components possess similar microgeometry, for example, a mixture of two liquids insoluble in one another, a mixture of fine powders after sintering, etc. It is commonly supposed that the Bruggeman geometry consists of intermixed components. Stroud anticipated [44] that the BE is most appropriate to a composite made up of uniform cells which all together fill the space completely and are compact and roughly spherically shaped. Irene believes that the equation ''may be appropriate for mixed phase films and large amounts of impurities in substrates and damage'' [10].

The problem of applicability of the BE is closely related to finding microgeometries for which this equation is realizable. Milton showed [45] that one of such microgeometries can be exactly realizable by some multiscale hierarchical microstructures where spheres of arbitrary dimension are well separated with self-similarity on all length scales. Considering disordered random resistor networks and applying a diagrammatic technique, Luck [46] found that the effective conductivity generically deviates from the BE at the fourth order of perturbation theory; on a square lattice, due to the duality symmetry, the BE becomes incorrect only in the fifth order. Finally, using a target optimization procedure, Torquato and Hyun [43] found that periodic arrays of generalized hypocycloidal inclusions arranged in a checkerboard pattern approximately achieve the BE.

At the same time, the BE has disadvantages that lead to its inapplicability in many cases. Here it is assumed that each polarizable cell is surrounded by the effective medium. The environment of a given cell is not really a fixed effective medium, however, but is variable. At high concentrations (and particularly near the percolation threshold) the above assumption can be poor. Indeed, isolated occupied sites, sites which are along a single strand path, sites surrounded by other occupied sites, and sites along a dead end branch are all in very different environments. In other words, the BE relies on the average field concept and completely neglects the local field fluctuations; this allows one to obtain an approximate analytical solution. Of course, as a statistical theory the BE ignores imperfect interface contact and boundary scattering, i.e., actual energy dissipation at boundaries due to interaction between current or heat carriers and defects or interfaces [47–52]. This problem, however, is outside our consideration.

It should be noted that the BE does not contain parameters signifying the system microgeometry. As a consequence the BE gives the fixed percolation threshold $f_c = 1/d$, where d is the space dimensionality. As we will see later, this value of p_c is, however, a rarity for natural and artificial heterosystems.

As noted earlier [53], the validity of the BE increases with decreasing dimensionality. This is due to the fact that as the dimensionality increases the opportunity for current flow around (or toward) a region of differing conductivity increases. Clearly, as the path around the component (cell) in question becomes more important, the fluctuations in this path also become more important.

*On leave from Institute of Semiconductor Physics, National Academy of Sciences of Ukraine, 45 prosp. Nauki, 03028 Kyiv, Ukraine.

Looking through the literature concerning generalizations of the BE we would like to note some papers which are, in our view, of interest. First of all, we note the contribution due to Granqvist and Hunderi [54,55]. They showed that it is possible to represent resonance frequencies of various configurations of identical touching spheres using one triplet of effective depolarization factors (L_i^*) which signifies an ellipsoidal shape. This means that a complex system of *interacting* spheres may be effectively replaced by a system of *noninteracting* ellipsoids. In addition, they also pointed out the crucial possibility of using a distribution of the depolarization factors to obtain the needed value of the critical exponent for conductivity.

McLachlan [56,57] and McLachlan, Blaskiewicz, and Newnham [58] considered some generalized versions of the BE written in terms of microgeometry parameters (the space dimensionality, critical volume fraction f_c, and critical exponent). The main idea was to relate effective medium theory to percolation theory. Thus their equations are some hybrid of both theories or a bridge connecting them.

Ghosh and Fuchs [59] proposed a theory for the dielectric response of rock-and-brine systems, based on the spectral representation with its sum rules. Starting with the spectral density function for the BE, they modified it and derived an analytical expression for the effective dielectric function of the composite. It is shown that the features common to the dielectric functions of many rock systems can be derived from the theory. In particular, it predicts static and/or dynamic scaling near the percolation threshold under appropriate conditions. Moreover, it is in quantitative agreement with the experimental data. However, the theory has three free parameters whose connection with the system microgeometry is, generally speaking, unclear.

Pecharroman and Iglesias [60] assumed both composite components to be randomly oriented spheroids. The expression obtained is a two-parameter generalization of the BE where the depolarization factors of the spheroids are free parameters. Alternatively, one of the depolarization factors and the percolation threshold can be considered as free parameters.

Dvoynenko *et al.* [61] treated the system dimensionality entering the BE as a free parameter varying near the percolation threshold where the correlation length is large. As a result, their model allows one to describe with reasonable accuracy the experimental transmittance spectra of semicontinuous gold films evaporated onto glass substrates.

In this report we develop another, unified approach based on the concept of a shape-distributed particle system. Preparatory to considering the BE in detail, we would like to mention this concept briefly. This issue may be of interest from two angles. On the one hand, real particle systems are usually shape distributed. From this standpoint it is of interest to consider, for example, assemblies of particles with a shape distribution to take into account its effects on the linear and nonlinear optical response [62–64]. On the other hand, the effective transport coefficients for any composite systems are the same as for a shape-distributed system of spheroids [65]. This is a direct and evident consequence of Bergman's theorem [66,67] (see also [59]). Thus we may consider a system of spheroids instead of the real composite system, which can be rather complex. We will return to this problem later, in our discussion. In Sec. II we consider the classical formalism by Bruggeman and Landauer. In Secs. III–IV we present various extensions of the BE using the concept of shape-distributed particle composites. A brief review and our discussion of the percolation threshold problem are given in Sec. V. Finally, in Sec. VI we discuss the results obtained and in Sec. VII sum up the results and give our concluding remarks.

II. CLASSICAL BRUGGEMAN-LANDAUER FORMALISM

The classical BE was pioneered by Bruggeman [1]. However, in our mind, a physically more correct derivation of this equation was given by Landauer [53,68]. In this theory a typical element of the two-phase composite is embedded in an effective medium. The properties of the medium, in turn, are to be determined self-consistently. To do this, it is necessary to solve for the local field around the element and impose the requirement that the local field fluctuations are zero on average.

Following Landauer's line of reasoning, let us consider a spherical inclusion with a conductivity σ_i and volume V and assume it is embedded in a uniform medium with an effective conductivity σ_{eff}. If the applied (far) field is E_0 then a dipole moment related to the volume under consideration is, in three dimensions (3D),

$$p_i = \frac{3V}{4\pi}\theta_i E_0, \tag{1}$$

where $\theta_i = (\sigma_i - \sigma_{\text{eff}})/(\sigma_i + 2\sigma_{\text{eff}})$ is the dimensionless sphere polarizability. This polarization produces a deviation from E_0. If the average deviation from E_0 is considered to vanish, the total polarization (summed over both elements of our composite) must vanish too. This leads to the well-known simple equation

$$f_1\theta_1 + f_2\theta_2 = 0, \tag{2}$$

where f_1 and f_2 are the filling factors (volume fractions) of phases 1 and 2, respectively. There is another way to obtain the classical BE, namely, one imposes the condition that the deviation of the current from the average must vanish [53].

Bruggeman's theory is trivially extendable to arbitrary dimensionality of the system. In this case we have to take in Eq. (2) [53]

$$\theta_i = \frac{\sigma_i - \sigma_{\text{eff}}}{\sigma_i + (d-1)\sigma_{\text{eff}}}, \tag{3}$$

where d is the system dimensionality.

Equation (2) is a quadratic equation and to be physically correct its solution has to be positive. If we deal with a multiphase composite system then Eq. (2) can obviously be generalized to

$$\sum_i f_i\theta_i = 0. \tag{4}$$

It should be noted that there is an algorithm based on conformal mapping allowing one to select the physically correct solution for this case [69].

The classical BE can be easily generalized to the case of typical elements of ellipsoidal shape. For the isotropic composite two methods of generalization are possible. If the ellipsoids are equally oriented and the electric field is directed along one of the ellipsoid axes, then (see, e.g., [70])

$$\theta_i=\frac{1}{3}\,\frac{\sigma_i-\sigma_{\rm eff}}{\sigma_{\rm eff}+(\sigma_i-\sigma_{\rm eff})L}, \tag{5}$$

where L is the ellipsoid depolarization factor corresponding to the direction of the above field [71]. If the ellipsoids are randomly oriented, then [55,70]

$$\theta_i=\frac{1}{3}\sum_{j=1}^{3}\frac{\sigma_i-\sigma_{\rm eff}}{\sigma_{\rm eff}+(\sigma_i-\sigma_{\rm eff})L_j}. \tag{6}$$

For the sake of convenience we introduce the designation

$$s_i=\frac{\sigma_{\rm eff}}{\sigma_i-\sigma_{\rm eff}}=\frac{\mu_{\rm eff}}{\mu_i-\mu_{\rm eff}}, \tag{7}$$

where μ is a transport coefficient. Then Eqs. (3) and (4) may be rewritten as

$$\sum_i f_i[1+ds_i]^{-1}=0. \tag{8}$$

Combining Eqs. (5) and (4) one obtains

$$\sum_i f_i[s_i+L]^{-1}=0. \tag{9}$$

At the same time, combining Eqs. (6) and (4) one obtains

$$\sum_i f_i\sum_{j=1}^{3}(s_i+L_j)^{-1}=0, \tag{10}$$

where the well-known condition for the ellipsoid depolarization factors

$$L_3=1-L_1-L_2 \tag{11}$$

has to be taken into account.

III. 1D DISTRIBUTIONS

A. General considerations

It would appear natural to consider a generalization of Eq. (9) of the form

$$\sum_i f_i\int_0^1 dL\,\frac{P(L)}{s_i+L}=0, \tag{12}$$

where $P(L)$ is a distribution function. Clearly, this function is to be normalized to unity,

$$\int_0^1 dL\,P(L)=1. \tag{13}$$

Let us consider the percolation properties of Eq. (12) for a two-phase composite medium. Usually the percolation problem is formulated in terms of the conductivity; we will also follow this rule. If σ_1 and σ_2 are the conductivities of the insulating and metallic phases, respectively, then we may write (see also [61]) $\sigma_{\rm eff}\ll\sigma_2$ or

$$s_2\cong 0 \tag{14}$$

below the percolation threshold, where there is no percolation, and $\sigma_1\ll\sigma_{\rm eff}$ or

$$s_1\cong -1 \tag{15}$$

above it, where percolation exists. Both conditions (14) and (15) have to hold at the percolation threshold. Substituting Eqs. (14) and (15) in Eq. (12), one has

$$(1-f_c)\int_0^1 dL\,\frac{P(L)}{L-1}+f_c\int_0^1 dL\,\frac{P(L)}{L}=0, \tag{16}$$

where f_c is the critical value of the metallic phase filling factor. Equation (16) may be rewritten as

$$\int_0^1 dL\,P(L)G(L)=0, \tag{17}$$

where

$$G(L)=\frac{L-f_c}{L(L-1)}. \tag{18}$$

Equations (17) and (18) signify an important condition connecting the critical filling factor with general 1D distributions of ellipsoidal shapes, and we will use them below. For further consideration we have to signify the form of the distribution function $P(L)$.

B. Distribution as two δ functions

It seems likely that the simplest nontrivial distribution deserving consideration is that as two δ functions, namely,

$$P(L)=\frac{1}{2}[\,\delta(L-L_1^*)+\delta(L-L_2^*)]. \tag{19}$$

To satisfy Eq. (17) we ought to take here (see Fig. 1)

$$G(L)=\frac{L-f_c}{L(L-1)}=\pm a, \tag{20}$$

which yields two solutions,

$$L_1^*=\frac{a+1-\sqrt{(1+a)^2-4af_c}}{2a} \tag{21}$$

and

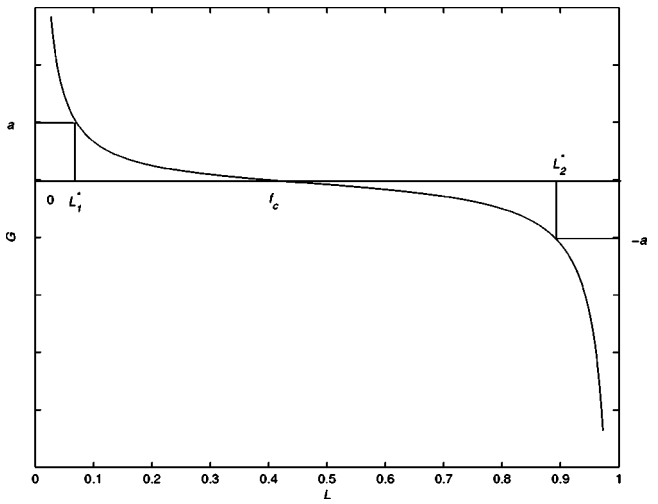

FIG. 1. Illustration for Eqs. (19)–(22).

$$L_2^* = \frac{a - 1 + \sqrt{(1-a)^2 + 4af_c}}{2a}. \tag{22}$$

After direct substitution of Eq. (19) into Eq. (12) one has the final equation for μ_{eff},

$$\frac{1-f}{s_1 + L_1^*} + \frac{1-f}{s_1 + L_2^*} + \frac{f}{s_2 + L_1^*} + \frac{f}{s_2 + L_2^*} = 0. \tag{23}$$

Earlier, a similar equation was derived by Pecharroman and Iglesias [60]. We note that Eq. (23) is a two-parameter equation and it describes a system consisting of particles of two kinds, namely, elongate and flattened spheroids for each phase. One of the parameters (a) shows how far the spheroid shapes deviate from spherical. The other parameter (f_c) is, as before, the critical filling factor. The degeneracy condition ($a \to 0$) yields a simpler one-parameter equation,

$$\frac{1-f}{s_1 + f_c} + \frac{f}{s_2 + f_c} = 0, \tag{24}$$

which is nothing more nor less than a combination of Eqs. (4) and (5) and will be considered by us as a particular case of Eq. (23). It should be noted that a similar equation was proposed by Xia, Hui, and Stroud [72] to calculate the optical properties of Faraday-active composites. Later, it was repeatedly used for description of the optical spectra of magnetic materials (see, e.g., [73,74]). At $f_c = 1/3$ Eq. (24) reduces to the classical BE. Davidson and Tinkham [75] take here $f_c = 1/6$ [see Eq. (45) below], which yields good agreement with experimental data for the effective conductivity of three metal-insulator composites.

C. Beta distribution

Let us now consider a rather general distribution, namely, the Beta distribution

$$P(L) = CL^{\alpha-1}(1-L)^{\beta-1}, \tag{25}$$

where $C = \Gamma(\alpha+\beta)/\Gamma(\alpha)\Gamma(\beta)$ is the normalization constant and $\Gamma(\cdots)$ is the gamma function.

The properties of this distribution are well known. In particular, its variance is

$$D(L) = \frac{\alpha\beta}{(\alpha+\beta)^2(\alpha+\beta+1)}. \tag{26}$$

At the same time, at various values of its parameters (α and β) the Beta distribution has radically different properties. As a result, many distributions may be approximated by this distribution.

Substituting Eq. (25) into Eq. (12) gives (see, e.g., [76])

$$\sum_i \frac{f_i}{s_i} B(\alpha,\beta)\, {}_2F_1\left(\alpha, 1; \alpha+\beta; -\frac{1}{s_i}\right) = 0, \tag{27}$$

where $B(\alpha,\beta)$ is the Beta function and ${}_2F_1(\cdots)$ is the hypergeometric function. It is easy to check that $f_c = 0$ for a system with such distribution. Obviously, this is because the Beta distribution possesses the following property: for any $L > 0$ (it goes without saying that $L \leqslant 1$), $P(L) > 0$. This means that there can be needles in the system under consideration as long as one likes. Thus, the system undergoes the percolation threshold at $f = 0$. In other words, for corresponding microgeometries a conductor retains conductivity until it is completely replaced by an insulator.

The distribution has two parameters. Varying in the interval [0;1], its parameters enable us to consider a wide class of composite microgeometries. Some particular cases of the Beta distribution admitting analytical solutions are considered below.

1. $\alpha = 1-\beta$

In this case we use the fact that [76]

$${}_2F_1(a,1;1;z) = (1-z)^{-a}, \tag{28}$$

and one obtains the one-parameter equation

$$\mu_{\text{eff}} = \mu_1\mu_2 \frac{(1-f)\mu_2^{\alpha-1} + f\mu_1^{\alpha-1}}{(1-f)\mu_2^{\alpha} + f\mu_1^{\alpha}}. \tag{29}$$

If now one takes $\alpha = 1/2$ then one obtains

$$\mu_{\text{eff}} = \mu_1 \frac{1 + f(\sqrt{\mu_2/\mu_1} - 1)}{1 + f(\sqrt{\mu_1/\mu_2} - 1)}. \tag{30}$$

Earlier this equation was considered in [77–79].

2. $\alpha = 2-\beta$

This case has been given adequate consideration in [80] (see also [81]). It reduces to the well-known and widely used Lichtenecker equation

$$\mu_{\text{eff}}^{1-\alpha} = \sum_i f_i \mu_i^{1-\alpha}, \tag{31}$$

where the single parameter α lies in the interval [0;2].

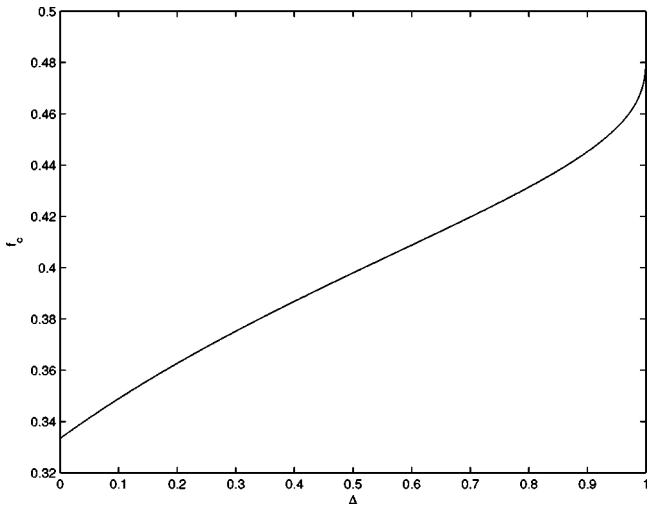

FIG. 2. Dependence $f_c(\Delta)$ calculated according to Eq. (37).

3. α=1/2, β=1

In this case we use the fact that [76]

$$ {}_2F_1\left(\frac{1}{2},1;\frac{3}{2};z^2\right)=\frac{1}{2}z^{-1}\ln\frac{1+z}{1-z}. \tag{32}$$

This yields the final equation

$$\sum_i f_i s_i^{1/2}\ln[1+2(s_i^{-1/2}-1)^{-1}]=0, \tag{33}$$

which, as far as we know, has not been used in the relevant literature yet.

D. Steplike distribution of spheroidal shapes

For a spheroid one can take (see, e.g., [62]) $L_1=L_2$ and $L=L_3=1-2L_1=1-2L_2$. Thus, for shape-distributed spheroids *equally* oriented along their revolution axis Eq. (12) can be rewritten as

$$\sum_i f_i\theta_i=\sum_i f_i\int_0^1 dLP(L)(s_i+L)^{-1}=0. \tag{34}$$

The simplest form of the distribution function that deserves attention in this case is the one-parameter steplike distribution [82,83]

$$P(L)=\frac{2}{\Delta^2}\chi\left(L-\frac{1}{3}+\frac{1}{3}\Delta\right)\chi\left(-L+\frac{1}{3}+\frac{2}{3}\Delta\right), \tag{35}$$

where $\chi(\cdots)$ is the Heaviside unit function and Δ is a parameter signifying nonsphericity. Direct integration yields

$$\theta_i=\frac{2}{\Delta^2}\ln\frac{s_i+1/3+(2/3)\Delta}{s_i+1/3-(1/3)\Delta}. \tag{36}$$

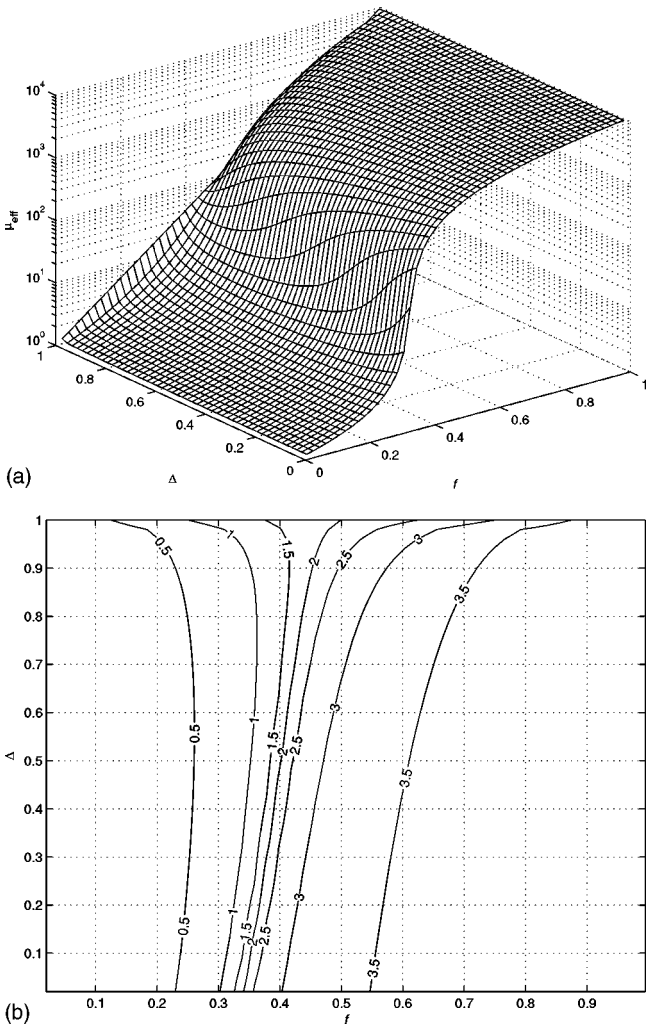

FIG. 3. (a) Surface $\mu_{\rm eff}(f,\Delta)$ calculated according to Eqs. (34)–(36). (b) Patterns of isolines $\log_{10}\mu_{\rm eff}(f,\Delta)$=const calculated according to Eqs. (34)–(36).

By applying Eqs. (14), (15), (34), and (36) to a two-phase composite ($i=2$), the equation for the critical filling factor may be written as

$$(1-f_c)\ln\frac{1-\Delta}{1+\Delta/2}+f_c\ln\frac{1+2\Delta}{1-\Delta}=0. \tag{37}$$

The solution of this equation is presented in Fig. 2. As may be seen, percolation can take place when $1/3<f<1/2$.

The dependence $\mu_{\rm eff}(f,\Delta)$ calculated according to Eqs. (34)–(36) for a two-phase composite is presented in Fig. 3(a); in order for the figure to be more dramatic we take here the transport coefficients of the phases as extremely different from one another, $\mu_2/\mu_1=10^4$. It is interesting also to construct the isolines $\log_{10}(\mu_{\rm eff})$=const [see Fig. 3(b)]. As may be seen, $\mu_{\rm eff}$ changes abruptly as the filling factor goes through its critical value (the values of $\mu_{\rm eff}$ are given on a logarithmic scale here). It should also be noted that, whereas the dependence $\mu_{\rm eff}(f)$ is always monotonic, the dependence $\mu_{\rm eff}(\Delta)$ is not. So at small f this function first decreases and

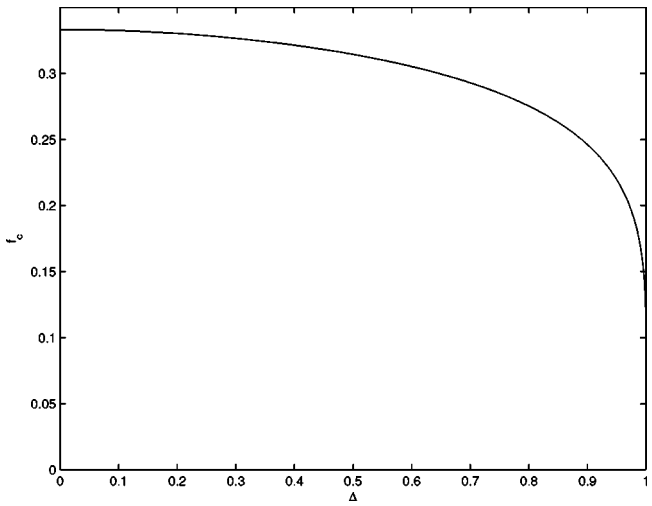

FIG. 4. Dependence $f_c(\Delta)$ calculated according to Eq. (41).

then rises. In contrast, at large f it decreases monotonically with increasing nonsphericity parameter Δ.

IV. 2D DISTRIBUTIONS

For an ellipsoid two depolarization factors are linearly independent. Thus for *randomly* oriented shape-distributed ellipsoids Eq. (10) can be rewritten as [84]

$$\sum_i f_i\theta_i=\sum_i f_i\int\int dL_1dL_2P(L_1,L_2)\sum_{j=1}^{3}(s_i+L_j)^{-1}=0, \tag{38}$$

where we have to take into account Eq. (11). The one-parameter steplike distribution for this case may be written as [64,65,85,86]

$$P(L)=\frac{2}{\Delta^2}\chi\left(L_1-\frac{1}{3}+\frac{1}{3}\Delta\right)\chi\left(L_2-\frac{1}{3}+\frac{1}{3}\Delta\right)\times\chi\left(-L_1-L_2+\frac{2}{3}+\frac{1}{3}\Delta\right). \tag{39}$$

Substitution of Eq. (39) into Eq. (38) yields after direct integration [85]

$$\theta_i=\frac{2}{\Delta^2}\left[\left(s_i+\frac{1}{3}+\frac{2}{3}\Delta\right)\ln\frac{s_i+1/3+(2/3)\,\Delta}{s_i+1/3-(1/3)\,\Delta}-\Delta\right]. \tag{40}$$

As before for spheroids, we consider first the percolation properties of a similar two-phase system of ellipsoids. By applying Eqs. (14), (15), (38), and (40) to the two-phase composite, the equation for the critical filling factor may be written as

$$2(1-f_c)(1-\Delta)\ln\frac{1+\Delta/2}{1-\Delta}+f_c(1+2\Delta)\ln\frac{1+2\Delta}{1-\Delta}=3\Delta. \tag{41}$$

Its solution is presented in Fig. 4. It is interesting that in this case the percolation can take place only when $f<1/3$.

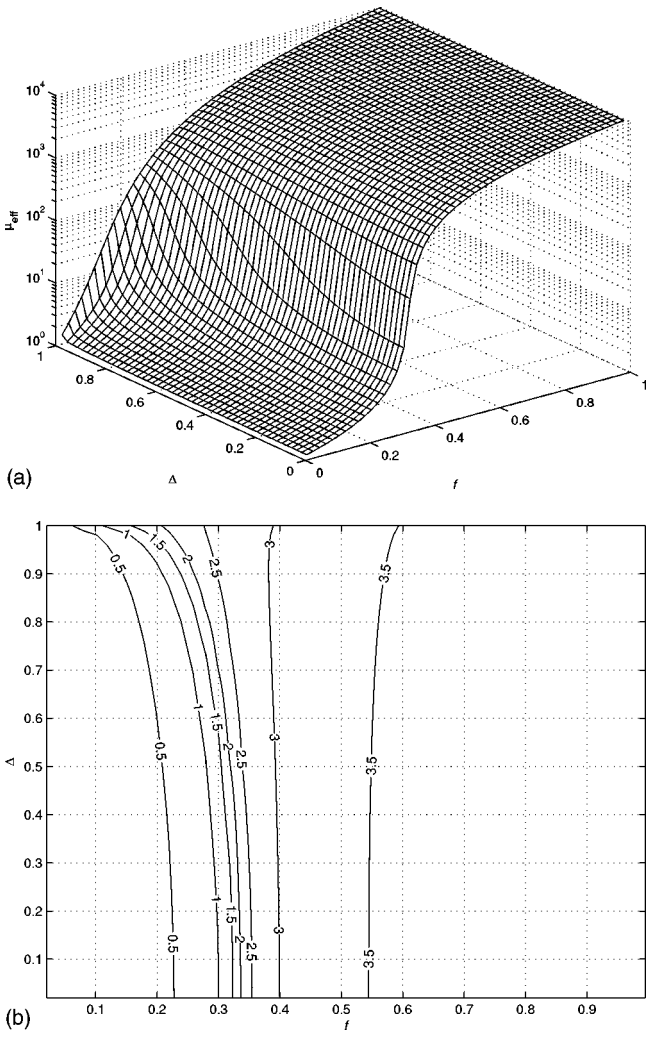

FIG. 5. (a) Surface $\mu_{\text{eff}}(f,\Delta)$ calculated according to Eqs. (38)–(40). (b) Patterns of isolines $\log_{10}\mu_{\text{eff}}(f,\Delta)$=const calculated according to Eqs. (38)–(40).

The dependence $\mu_{\text{eff}}(f,\Delta)$ calculated according to Eqs. (38)–(40) for the two-phase composite and the isolines $\log_{10}(\mu_{\text{eff}})$=const at $\mu_2/\mu_1=10^4$ are presented in Figs. 5(a) and 5(b), respectively. As may be seen, the function μ_{eff} changes abruptly as the filling factor goes through its critical value. At small f the function rises monotonically with the nonsphericity parameter Δ; at large f it decreases with it. At some intermediate f (about 0.4) it depends almost not at all on this parameter.

Of course, many variants exist for choosing the shape distribution function of randomly oriented ellipsoids. For example, one can choose the generalized Beta distribution

$$P(L_1,L_2)=\text{const}\times L_1^{\alpha-1}(1-L_1)^{\beta-1}L_2^{\alpha-1}(1-L_2)^{\beta-1}\times(1-L_1-L_2)^{\alpha-1}(L_1+L_2)^{\beta-1} \tag{42}$$

or the generalized steplike distribution [65]

$$P(L_1,L_2)=\text{const}\times\left\{\frac{\pi}{2}+\arctan\left[a\,\frac{-L_1+1/3-\Delta/3}{L_1(L_1-1)}\right]\right\}\times\left\{\frac{\pi}{2}+\arctan\left[a\,\frac{-L_2+1/3-\Delta/3}{L_2(L_2-1)}\right]\right\}\times\left\{\frac{\pi}{2}+\arctan\left[a\,\frac{-L_1-L_2+2/3+\Delta/3}{(1-L_1-L_2)(L_1+L_2)}\right]\right\}. \tag{43}$$

We note, however, that neither of the above distributions provides a nonzero percolation threshold, for the same reasons discussed in Sec. III C for the Beta distribution.

V. PERCOLATION THRESHOLD

As we see, the percolation threshold is the important parameter in our consideration. It is well known also that percolation processes play a major part in the physics and chemistry of composites, helping to describe the overall dependence of various transport properties on the microgeometry. At the same time, it is our opinion that there exists a lot of misunderstanding related to this issue. Because of this, we will consider the problem of the percolation threshold in more detail.

The percolation problem is versatile and complex by itself. On the one hand, there are some general approaches and models allowing one to calculate the percolation threshold in various situations. On the other hand, many situations exist that have defied explanations within the framework of these approaches; to be specific, we shall present some examples below.

The well-known work of Scher and Zallen [87,88] considers the problem of *site* percolation on lattices; another problem of lattice percolation, known as the *bond* percolation problem, reduces to the above problem, but on a different lattice (see also [89,90] and references therein). In particular, for the site percolation problem on a lattice these authors proposed that the critical fraction of sites is to be an invariant when expressed as a filling (volume) factor, depending on dimensionality only. Because f_c is approximately universal, i.e., essentially independent of the lattice structure, they suggested that it may be carried into continuum systems. So the critical filling factors

$$f_c\cong 0.45 \tag{44}$$

[some other estimations give $f_c\cong 0.5$ (see, e.g., [58])] in 2D and

$$f_c\cong 0.16 \tag{45}$$

in 3D were found to be invariant. Later, a similar approach was repeatedly applied to continuum percolation problems. Below we will see that some experimental work approximately supports these results and some does not. At present it is believed that Eq. (45) is valid for such hard (impermeable) spheres of a single size that nearest neighbors just touch, situated randomly on all lattices in 3D, as well as for random closely packed systems. At the same time, the theory of continuum percolation has evolved in different directions (see, e.g., [91–94] and references therein). One approach showing considerable promise [95–97] uses a mapping between the continuum percolation model and the so-called Potts fluid [98]. The authors of [97] suggest, in particular, that their model can be useful to describe microemulsions and composite materials. We note that the percolation threshold (in this theory one calls it the critical density of interacting particles) is not universal but is sensitive to all the details of the system under consideration [97].

The Scher-Zallen approach is shown to be applicable only for clusters built up of hard (nonoverlapping) particles. The phenomenological continuum percolation theory for overlapping objects is developed, particularly, in [99–101]. These authors discuss percolation in 2D and 3D, using the model of randomly oriented overlapping holes of various shapes and ellipsoids of revolution. They noted [100] some important materials science applications of their model, such as crack formation, sintering ceramic powders, and hydrating cement-based materials; a good review of the percolation theory applied to concrete is given by Garboczi [102]. We would like to note three important conclusions made by the authors of [99–101] on the basis of their computer simulations.

(i) In 2D, the percolation threshold for identical overlapping ellipses with aspect ratio η, whose centers and orientations are random, can be well fitted to the formula

$$f_c=3^{\,4/(2+\eta+1/\eta)}. \tag{46}$$

In particular, for circles this yields

$$f_c=1/3. \tag{47}$$

(ii) Of all objects of a given volume, the sphere has the maximum percolation threshold for overlapping objects. In 3D this threshold

$$f_c\cong 0.29. \tag{48}$$

(Interestingly, another percolation algorithm for overlapping spheres, the so-called Swiss-cheese model, on a simple cubic lattice yields [103]

$$f_c\cong 0.034. \tag{49}$$

It is considered to be useful for description of sandstones and some other porous systems.)

(iii) In 3D, even for simple overlapping shapes, the dependence of the percolation threshold cannot be completely described by single-particle shape functionals.

Interestingly, we do not know of any published work on the percolation threshold of shape-distributed particle systems despite the fact that such systems are doubtless of practical interest. Moreover, most studies cover the percolation of equal-sized constituents only. There are only fragmentary data on percolation in polydisperse systems (see, e.g., [104] and references therein).

Let us now consider some experimental results concerning the percolation threshold in composite media. At present there are comprehensive data on percolation properties of thin films. Semicontinuous metallic films obtained by vari-

ous methods of deposition on dielectric substrates may be considered as quasi-2D. For thin gold films made at room temperature by electron-beam evaporation onto amorphous Si_3N_4 windows, the percolation threshold is found to be $f_c \cong 0.74$ [105]. At the same time, $f_c \cong 0.71$ for thin gold films deposited by thermal evaporation at room temperature on an amorphous substrate, and $f_c \cong 0.53$ for those deposited on a polycrystalline substrate [106]. Other results [61] give $f_c \cong 0.75$ for gold films deposited on glass at high temperature and $f_c \cong 0.56$ for those deposited at low (room) temperature. For copper films thermally evaporated onto quartz-glass substrates, Dobierzewska-Mozrzymas *et al.* [107] obtained $f_c \cong 0.63$. In recent experiments by Seal *et al.* [108], $f_c \cong 0.65$ for semicontinuous silver films on dielectric substrates obtained by laser ablation.

Relatively thick (Cermet) films obtained by cosputtering (or coevaporating) metals with insulators may be considered as quasi-3D. Here we would like to note the results of Abeles *et al.* for W-Al_2O_3 Cermet films [109] ($f_c \cong 0.47$), Barzilai *et al.* for Co-SiO_2 Cermets [110] ($f_c \cong 0.55$), and Niklasson and Granqvist for Co-Al_2O_3 Cermets [111] ($f_c \cong 0.25$). For Ni-MgO composites obtained by coprecipitation of NiO-MgO solid solutions and their preferential reduction in a hydrogen atmosphere, $f_c \cong 0.32$ [112]. For amorphous carbon-Teflon composites obtained by mixing and compressing initial fine powders, the estimated value of the percolation threshold is $f_c \cong 0.29$ [113]. For $YBa_2Cu_3O_{7-\delta}$/CuO composites $f_c \cong 0.18$ [114]. For carbon-wax mixtures exhibiting the tunneling mechanism of conductivity, $f_c \cong 0.1$ [115], and for filamentary nickel $f_c \cong 0.075$ [116]. Finally, for graphite-hexagonal boron nitride powder mixtures Wu and McLachlan obtained $f_c \cong 0.12-0.15$ [117]. In addition, they noted that the values of f_c are typically 0.11–0.125 in the powders.

The authors of many of the above works advance various arguments to justify why their values of the percolation threshold differ from the theoretical ones. Some considerations of how to achieve either a very low or a high percolation threshold and some practical examples are given by McLachlan [118]. We would like, however, to note the following. There is no question that the percolation threshold is a nonuniversal parameter explicitly depending not only on dimensionality but on the system microgeometry (on the type of the percolation system considered) as well; generally speaking, it is sensitive to all the details of the system and may be between zero and unity. It is a challenging task to predict beforehand the percolation threshold for a composite system under study. In our view, however, a problem exists which can be formulated as follows. Due to the diversity of composite systems, both natural and artificial, they can have various microgeometries and exhibit various percolation mechanisms. Hence, it is of value to catalog the main types of such microgeometries and to study the corresponding mechanisms. It looks as if there is still a long way to go to solve the above problem.

VI. DISCUSSION

The results reported here demonstrate that the choice of the shape distribution function can lead to widely different

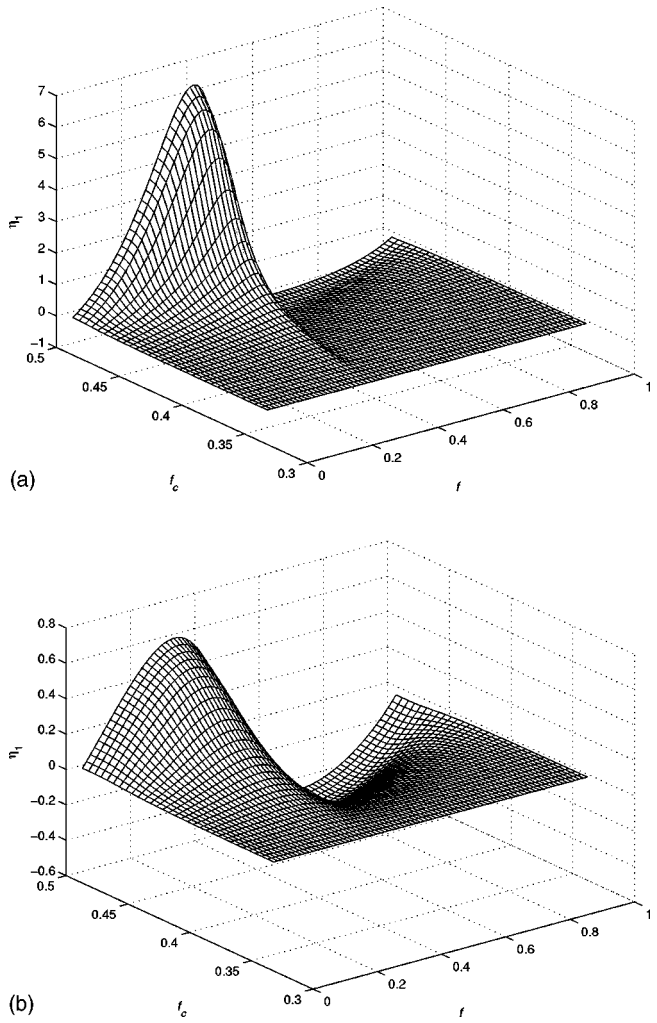

FIG. 6. Relative change of the effective transport coefficients $\eta_1(f,f_c)$ at $\mu_2/\mu_1=$(a) 10^4; (b) 10^2.

homogenization theories. We have obtained, in particular, certain one-parameter as well as two-parameter generalizations of the classical BE. Obviously, the simplest generalization is that signified by Eq. (24). Its properties are identical with those of the classical BE, but the critical (threshold) filling factor is a free parameter here. So it is interesting to compare the numerical results for $\mu_{\rm eff}$ obtained using Eq. (24) and our other approximations. Because the use of the Beta distribution (see Sec. III C) yields no nontrivial percolation threshold, we consider some results obtained with the use of Eq. (34) supplemented with Eq. (36), and with the use of Eq. (38) supplemented with Eq. (40). So in Figs. 6 and 7 we show the dependences $\eta_1(f,f_c)=(\mu'_{\rm eff}-\mu^*_{\rm eff})/\mu^*_{\rm eff}$ and $\eta_2(f,f_c)=(\mu''_{\rm eff}-\mu^*_{\rm eff})/\mu^*_{\rm eff}$, where $\mu^*_{\rm eff}$, $\mu'_{\rm eff}$, and $\mu''_{\rm eff}$ are calculated using Eqs. (24), (34)–(36), and (38)–(40), respectively. We see that in the case of a very high (very low) ratio of the phase transport coefficients [at $\mu_2/\mu_1=10^4$, Fig. 6(a)], Eqs. (24) and (34) can yield radically different values of the effective transport coefficients, especially close to the point $f_c=1/2$, where the nonsphericity parameter Δ is large. If the ratio is not so high [at $\mu_2/\mu_1=10^2$, see Fig. 6(b)], the difference between the values of $\mu_{\rm eff}$ is not large either. As

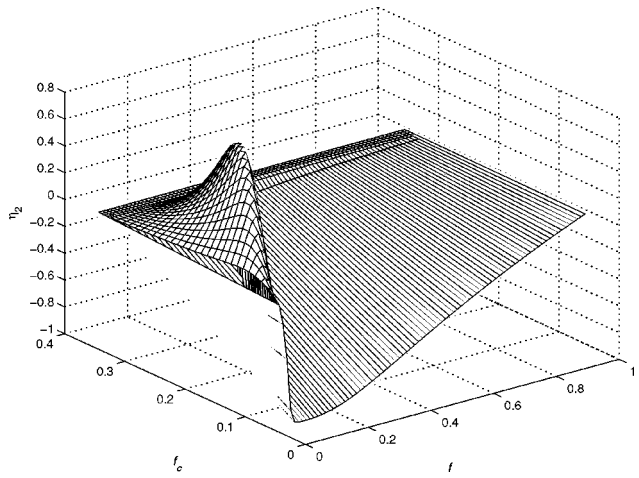

FIG. 7. Relative change of the effective transport coefficients $\eta_2(f,f_c)$ at $\mu_2/\mu_1=10^4$.

for Eq. (38), it does not yield very high values of η_2 even at $\mu_2/\mu_1=10^4$ (see Fig. 7). One should note also an interesting distinction between our models based on Eqs. (34)–(36) and on Eqs. (38)–(40). While consideration of equally oriented shape-distributed spheroids [Eqs. (34)–(36)] leads to increasing the percolation threshold relative to the case of the classical BE for spheres [Eq. (2)] where $f_c\cong 1/3$, consideration of randomly oriented shape-distributed ellipsoids [Eqs. (38)–(40)] leads to its decrease; so the value $f_c\cong 0.16$ [see Eq. (45)] is reached at $\Delta\cong 0.993$. In connection with this one can note the work of Sherwin *et al.* [119]. They considered the percolation threshold problem for *identical* parallel metallic ellipsoids in an insulator host with similar geometry using the Bruggeman formalism. In particular, their results show that for the direction along the longest principal semiaxis of spheroids the percolation threshold value is low for prolate spheroids and increases as the length of this semiaxis decreases relative to the lengths of the other two semiaxes. So the percolation threshold can be high for strongly oblate spheroids. This means that the percolation threshold for identical similarly oriented ellipsoids can increase as well as decrease relative to that for spheres.

What are the physical meaning and the importance of the approximation signified by Eqs. (34), (36), and (40)? At first glance it would seem that they describe some abstract and unlikely microgeometries, and so their importance is limited. Indeed, for corresponding microgeometries the effective medium is one where each ellipsoid is surrounded by a mixture of the two components (phases) that has the effective value of the medium. This means that the ellipsoids are of an infinite range in size, and that the larger ellipsoids are separated by a medium containing smaller ones. Moreover, the ellipsoids are distributed in shape. In fact, however, the geometry of actual composite systems is not necessarily so complex. The above microgeometries are only models admitting a simple mathematical description and their parameters are not directly related to the real shapes of the particles. One might note some distinguishing features of these models.

(1) The classical BE, as well as its generalizations considered here, are completely mean-field equations, not taking into account fluctuations of the local fields, and interactions among phases are represented by a constant (averaged) far field. However, they indirectly take into account higher multipole interactions. Needless to say, an exact calculation of the interactions in random composite systems containing complex-shaped phases is intractable. The multipole interaction is of particular value at high concentrations and near the percolation threshold due to the significant clustering of conducting and insulating areas. Granqvist and Hunderi [54] described this situation by incorporating dipole-dipole interactions (which are the most important of the multipole interactions) locally using the ellipsoid effective depolarization factors. In other words, in their treatment the shape- and interaction-governed effects on the effective transport coefficients are similar and consonant. Similar to the work by McLachlan [56,57], we consider the percolation threshold as a free parameter that enables one to circumvent the corresponding difficulties and impose the needed percolation threshold value.

(2) Our models cover a wide range of composite systems whose percolation threshold can vary from 0 to 1/2. As discussed earlier (see Sec. V), the percolation threshold of most studied 3D composites lies within that interval [120]. Actually, our model equations (36) and (40) are derived for 3D composite systems. Indeed, we have chosen the shape distribution function in such a manner that it is centered at the point $L=1/3$ (or $L_1=L_2=1/3$) which corresponds to the percolation threshold of the classical BE in 3D. At the same time, our approach is easily extended to 2D composites. To do this we ought to center our shape distribution function (which has to be one dimensional in this case) at the point $L=1/2$, which corresponds to the percolation threshold of the 2D classical BE.

(3) It goes without saying that our equations do not take into account such phenomena as scattering at interfaces and tunneling of carriers. One of the phenomenological approaches to the scattering problem lies in *renormalization* of the phase transport coefficients. To account roughly for quantum mechanical tunneling one can increase the effective volume of the conductive phase [121].

(4) Obviously, the key question of our consideration is the area of applicability of our approach. On the face of it, because we have chosen the function P to be the same for all phases, our consideration is valid only for geometries that rank among the so-called aggregate ones. Following Lamb *et al.* [122], we distinguish aggregate composite topology as that where all phases occur on an equal footing; for this topology the microgeometries of phases are similar. In contrast, for another type of topology (*cermet* topology), the phase microgeometries are different; there, particles of one phase (inclusions) are completely surrounded by another phase (host).

According to Bergman [66,67], for any two-phase macrohomogeneous system $\mu_{\rm eff}$ may be represented as

$$\mu_{\rm eff}=\mu_1\left\{1+f_2\int_0^1 dL g(L)[(\mu_2/\mu_1-1)^{-1}+L]^{-1}\right\}, \tag{50}$$

where $g(L)$ is the so-called spectral density function satisfying the sum rules

$$\int_0^1 dLg(L)=1 \quad \text{and} \quad \int_0^1 dLLg(L)=(1-f_2)/3. \quad (51)$$

The spectral density function does not depend on the material constants μ_1 and μ_2 and describes the microgeometry of a composite. Since it gives the spectrum of configurational resonances, it contains all geometrical information about the composite. At the same time, depending on the filling factor, it signifies the interactions inside the system. Thus the representation (50) allows one to separate the effects of microgeometry and material constants on the effective transport coefficients. Let us now formulate two important statements which, it seems, loom large in the effective medium theory.

Statement 1. The effective transport coefficients of any composite system are the same as those of a cermet composite system with the same material parameters.

This statement is a direct consequence of the above Bergman theorem (see, e.g., [65,83]). Indeed, in terms of electrodynamics the factor $[(\mu_2/\mu_1-1)^{-1}+L]^{-1}$ in Eq. (50) is simply the dipole polarizability of a spheroid with the depolarization factor L. The function $g(L)$ signifies the distribution of the spheroids in shape. Thus natural modes (resonances) of a composite may be expressed in terms of natural modes of small variously shaped spheroids. In other words, a diagonal component of the tensor μ_{eff} of the two-phase composite is the same as for a system of equally oriented noninteracting spheroids (here, the orientation of the applied electric field has to correspond to the revolution axis of the spheroids). We note that Eq. (50) is written for cermet topology where the phases 1 and 2 are host and inclusions, respectively. Consequently, two composites having different topologies can have the same effective transport coefficients. For example, a typical aggregate composite described by the classical BE has the same effective transport coefficients as a cermet composite with a known spectral density function [59].

Statement 2. Some (cermet) composite systems exist such that their effective transport coefficients differ from those of *any* aggregate composite system with the same material parameters.

This means that Eqs. (12) and (38) are not always applicable. One can suppose, for example, that they are inapplicable in the case of a dilute suspension of spheres for which (see, e.g., [83])

$$\mu_{\text{eff}}=\mu_1\left[1+3f_2\frac{\mu_2-\mu_1}{\mu_2+2\mu_1}\right]. \quad (52)$$

In other words, in a sense the aggregate topologies are a subset of cermet topologies. Indeed, we have assumed that the function $P(L)$ is the same for all phases, and hence the phase microgeometries are similar. At the same time, it would be more natural to suppose that each phase has its own function $P(L)$. So Eq. (12) is rewritten as

$$\sum_i f_i \int_0^1 dL \frac{P_i(L)}{s_i+L}=0. \quad (53)$$

From the above discussion one can suppose that our representation (12) and Bergman's representation (50) are not equivalent. Strictly speaking, the applicability area of Eqs. (12) and (38) has been something of a mystery; we believe that this problem will be considered in more detail elsewhere. At the same time, the shape distribution function P as well as the spectral density function g signify the microgeometry of the composite. In addition, they signify the interactions inside it; in doing so they signify them in different ways. We note that, owing to the simple form of the spectral density function g Eq. (50) might be more suitable for composites with Maxwell-Garnett-like microgeometry [64,65], while, owing to the simple form of the shape distribution function P, Eqs. (12) and (38) might be more suitable for composites with Bruggeman-like microgeometry. Thus, one advantage of the approach is that it suggests extensions for a wide class of composites based on some free topological parameters.

VII. CONCLUDING REMARKS

This report is written to present our main idea (the use of the concept of shape-distributed particle systems) in such a way as to be accessible to the researchers in various fields. Following this line of attack, we considered generalizations of the well-known classical BE in 3D. To demonstrate the efficiency of our approach, we showed that various assumptions for the shape distribution function yield many known equations for the effective transport coefficients. At the same time, to develop the approach used we proposed two other simple distributions for spheroidal and ellipsoidal shapes. This enabled us to obtain two one-parameter equations of the effective medium theory whose parameters signify the percolation threshold of the composite systems under consideration.

What are the future trends of our approach? Considering transport and relaxation in porous media, Hilfer [123] noted that almost all corresponding studies are motivated by one central question: How are the effective transport parameters influenced by the microscopic geometric structure of the medium? In our opinion, however, two problems, as applied to our situation, can be considered independently of one another, namely, (i) if we know what our composite microgeometry is then we can try constructing the corresponding function P; and (ii) if we know what the function P for an actual composite system is, we can try finding the corresponding microgeometry. In other words, our problem is to find the relationship between the shape distribution function and microgeometry of particular kinds of composites.

It seems reasonable to apply the following approaches to the above problems.

(1) Since some composite systems can be generated artificially, their optical properties can be measured in a wide frequency range using laboratory experiments. In principle, this makes it possible to solve the inverse problem

of determining the shape distribution function P for such systems directly from experimental data. A similar problem for the spectral density function $g(L)$ has already been considered (see, e.g., [124–126]).

(2) *Direct fitting based on some intuitive assumptions*. Frequently, one cannot extract the needed function from experimental data because the latter can be limited by a narrow spectral region or not be informative enough. In some cases, however, starting from *a priori* assumptions concerning properties of the shape distribution function, one can try to signify their general analytical form and determine the model parameters. For instance, some models for the function $g(L)$ were proposed in [127,128].

(3) *Numerical modeling with further fitting*. Some homogenization theories are based on numerical modeling. There are some examples [129] where the internal fields are calculated numerically for various problems, thus enabling one to compute the effective transport coefficients. Another example is the renormalized cluster expansion [130]. Using the corresponding numerical algorithms, one can find the required functions P for the problem under consideration.

(4) Finally, since some actual microgeometries are close to those corresponding to the well-known approximations, an opportunity exists to generalize the corresponding functions P which are known, say, for such approximations as the Bruggeman and Lichtenecker ones. As indicated above, Ghosh and Fuchs [59] applied this approach to the spectral density function g using Bergman's formalism. In the present work the formalism of the shape distribution function is used, a conceptual alternative for Bergman's formalism.

ACKNOWLEDGMENTS

The author wishes to thank Professor Kwang S. Kim for a helpful critical reading of an earlier version of this paper, as well as for his all-round support. This work is supported, in part, by MOST/KISTEP (CRI).

[1] D.A.G. Bruggeman, Ann. Phys. (Leipzig) **24**, 636 (1935).
[2] L.K.H. van Beek, in *Progress in Dielectrics*, edited by J.B. Birks (Heywood, London, 1967), Vol. 7, p. 69.
[3] A. Heilmann, G. Kampfrath, and V. Hopfe, J. Phys. D **21**, 986 (1988).
[4] R.W. Collins, Mater. Sci. Forum **52&53**, 341 (1989).
[5] W.M. Robertson, G. Arjavalingam, and S.L. Shinde, J. Appl. Phys. **70**, 7648 (1991).
[6] T. Olson and M. Avellaneda, J. Appl. Phys. **71**, 4455 (1992).
[7] J.T. Remillard, W.H. Weber, J.R. McBride, and R.E. Soltis, J. Appl. Phys. **71**, 4515 (1992).
[8] M. Fujii, M. Wada, S. Hayashi, and K. Yamamoto, Phys. Rev. B **46**, 15 930 (1992).
[9] R. Kampia and A. Lakhtakia, J. Phys. D **25**, 1390 (1992).
[10] E.A. Irene, Thin Solid Films **233**, 96 (1993).
[11] Z.Q. Wang, D. Stroud, and S.A. Dregia, Phys. Rev. B **50**, 12 073 (1994).
[12] C. Beleznay, D.A. Jelski, L. Nanai, and T.F. George, Fullerene Sci. Technol. **2**, 313 (1994).
[13] L.M. Schwartz, Physica A **207**, 131 (1994).
[14] B. Johs, R.H. French, F.D. Kalk, W.A. McGaham, and J.A. Woollam, Proc. SPIE **2253**, 1098 (1994).
[15] U. Rossow, U. Frotscher, C. Pietryga, W. Richter, and D.E. Aspnes, Appl. Surf. Sci. **102**, 413 (1996).
[16] R.W. Boyd, R.J. Gehr, G.L. Fischer, and J.E. Sipe, Pure Appl. Opt. **5**, 505 (1996).
[17] M. Schubert, B. Rheinlander, E. Franke, H. Neumann, T.E. Tiwald, J.A. Woollam, J. Hahn, and F. Richter, Phys. Rev. B **56**, 13 306 (1997).
[18] T.S. Sathiaraj and R. Thangaraj, J. Phys. D **30**, 769 (1997).
[19] R.W. Collins, D.E. Aspnes, and E.A. Irene, in *Spectroscopic Ellipsometry, Proceedings of the 2nd International Conference on Spectroscopic Ellipsometry* (Elsevier, Amsterdam, 1998).
[20] S.P. Friedman, Water Resour. Res. **34**, 2949 (1998).
[21] J.-G. Yoon, H.K. Oh, and Y.J. Kwag, J. Korean Phys. Soc. **33**, 699 (1998).
[22] N. Dmitruk, T. Lepeshkina, M. Pavlovska, and L. Zabashta, Nanostruct. Mater. **12**, 295 (1999).
[23] E. Dobierzewska-Mozrzymas, J. Wojcik, P. Bieganski, and E. Pieciul, Vacuum **54**, 289 (1999).
[24] S. Charvet, R. Madelon, F. Gourbilleau, and R. Rizk, J. Lumin. **80**, 257 (1999).
[25] P.M. Hui, X. Zhang, A.J. Markworth, and D. Stroud, J. Mater. Sci. **34**, 5497 (1999).
[26] I. Ohlidal and D. Franta, Acta Phys. Slov. **50**, 489 (2000).
[27] H. Song, W.J. Kim, and S.-J. Kwon, J. Magn. Magn. Mater. **213**, 126 (2000).
[28] J.D. Shane, T.O. Mason, H.M. Jennings, E.J. Garboczi, and D.P. Bentz, J. Am. Ceram. Soc. **83**, 1137 (2000).
[29] D.G. Kurth, P. Lehmann, D. Volkmer, A. Muller, and D. Schwahn, J. Chem. Soc. Dalton Trans. **2000**, 3989.
[30] M.I. Strashnikova, V.L. Voznyi, V.Ya. Reznichenko, and V.Ya. Gayvoronskii, Zh. Eksp. Teor. Fiz. **120**, 409 (2001) [J. Exp. Theor. Phys. **93**, 363 (2001)].
[31] M.I. Vasilevskiy, A.G. Polo, M.V. Artemiev, S.A. Filonovich, M.J.M. Jomes, and Yu.P. Rakovich, Phys. Status Solidi B **224**, 599 (2001).
[32] M. Nagai, R. Shimano, and M. Kuwata-Gonokami, Phys. Rev. Lett. **86**, 5795 (2001).
[33] A. Birner, R.B. Wehrspohn, U.M. Gosele, and K. Busch, Adv. Mater. (Weinheim, Ger.) **13**, 377 (2001).
[34] G.W. Petty and W. Grant, J. Appl. Meteorol. **40**, 2115 (2001).
[35] M. Wu, X. Yao, J. Zhai, and L. Zhang, Meas. Sci. Technol. **12**, 1932 (2001).
[36] M. Wu, H. Zhang, X. Yao, and L. Zhang, J. Phys. D **34**, 889 (2001).

[37] N.L. Dmitruk, T.A. Mikhailyk, and V.R. Romaniuk, Phys. Chem. Solid State **2**, 179 (2001).
[38] P. Facci, D. Alliata, L. Andolfi, B. Schnyder, and R. Kotz, Surf. Sci. **504**, 282 (2002).
[39] O. Dürr, W. Dieterich, P. Maass, and A. Nitzan, J. Phys. Chem. B **106**, 6149 (2002).
[40] R. Hill, J. Mech. Phys. Solids **13**, 213 (1965).
[41] J. Korringa, J. Math. Phys. **14**, 509 (1973).
[42] D.S. Wilkinson, W. Pompe, and M. Oeschner, Prog. Mater. Sci. **46**, 379 (2001).
[43] S. Torquato and S. Hyun, J. Appl. Phys. **89**, 1725 (2001).
[44] D. Stroud, Phys. Rev. B **19**, 1783 (1979).
[45] G.W. Milton, Commun. Math. Phys. **99**, 463 (1985).
[46] J.M. Luck, Phys. Rev. B **43**, 3933 (1991).
[47] G.W. Milton and N. Phan-Thien, Proc. R. Soc. London, Ser. A **380**, 305 (1982).
[48] S. Torquato, Appl. Mech. Rev. **44**, 37 (1991).
[49] S. Torquato and M.D. Rintoul, Phys. Rev. Lett. **75**, 4067 (1995).
[50] C.-W. Nan, R. Birringer, D.R. Clarke, and H. Gleiter, J. Appl. Phys. **81**, 6692 (1997).
[51] U. Kreibig, G. Bour, A. Hilger, and M. Gartz, Phys. Status Solidi A **175**, 351 (1999).
[52] C.M. Kleinlogel and L.J. Gauckler, J. Electroceram. **5**, 231 (2000).
[53] R. Landauer, in *Electrical Transport and Optical Properties of Inhomogeneous Media*, edited by J.C. Garland and D.B. Tanner, AIP Conf. Proc. No. 40 (AIP, New York, 1978), pp. 2–43.
[54] C.G. Granqvist and O. Hunderi, Phys. Rev. B **18**, 1554 (1978).
[55] C.G. Granqvist and O. Hunderi, Phys. Rev. B 18, 2897 (1978).
[56] D.S. McLachlan, J. Phys. C **20**, 865 (1987).
[57] D.S. McLachlan, Solid State Commun. **72**, 831 (1989).
[58] D.S. McLachlan, M. Blaskiewicz, and R.F. Newnham, J. Am. Ceram. Soc. **73**, 2187 (1990).
[59] K. Ghosh and R. Fuchs, Phys. Rev. B **38**, 5222 (1988).
[60] C. Pecharroman and J.E. Iglesias, Phys. Rev. B **49**, 7137 (1994).
[61] M.M. Dvoynenko, A.V. Goncharenko, V.R. Romaniuk, and E.F. Venger, Physica B **299**, 88 (2001).
[62] P. P'Neill and A. Ignatiev, Phys. Rev. B **18**, 6540 (1978).
[63] A.V. Goncharenko, V.V. Popelnukh, and E.F. Venger, J. Phys. D **35**, 1833 (2002).
[64] L. Gao, Phys. Lett. A **309**, 435 (2003).
[65] A.V. Goncharenko, V.Z. Lozovski, and E.F. Venger, J. Phys.: Condens. Matter **13**, 8217 (2001).
[66] D. Bergman, Phys. Rep., Phys. Lett. **43**, 377 (1978).
[67] D. Bergman, Ann. Phys. (N.Y.) **138**, 78 (1982).
[68] R. Landauer, J. Appl. Phys. **23**, 779 (1952).
[69] R. Jansson and H. Arwin, Opt. Commun. **106**, 133 (1994).
[70] D. Polder and J.H. van Santen, Physica (Utrecht) **12**, 257 (1946).
[71] Strictly speaking, the geometry corresponding to this case is anisotropic. So it would be more correct to say that Eqs. (4) and (5) give a diagonal component of the effective conductivity [65]. However, a formal transfer to the isotropic case is possible if all (diagonal) components of the effective conductivity tensor are considered to be signified in the same manner.
[72] T.K. Xia, P.M. Hui, and D.S. Stroud, J. Appl. Phys. **67**, 2736 (1990).
[73] E. Ganshina, A. Granovsky, V. Gushin, M. Kuzmichov, P. Podrugin, A. Kravetz, and E. Shipil, Physica A **241**, 45 (1997).
[74] H.R. Khan, A. Granovsky, F. Brouers, E. Ganshina, J.P. Clerc, and M. Kuzmichev, J. Magn. Magn. Mater. **183**, 127 (1998).
[75] A. Davidson and M. Tinkham, Phys. Rev. B **13**, 3261 (1976).
[76] F. Oberhettinger, in *Handbook of Mathematical Functions with Formulas, Graphs and Mathematical Tables*, Natl. Bur. Stand. Appl. Math. Ser. No. 53, edited by M. Abramovitz and I.A. Stegun, (U.S. GPO, Washington, DC, 1964).
[77] J.A. del Rio, R.W. Zimmerman, and R.A. Dawe, Solid State Commun. **106**, 183 (1998).
[78] L. Gao and J.Z. Gu, J. Phys. D **35**, 267 (2002).
[79] L. Gao, Phys. Lett. A **309**, 407 (2003).
[80] T. Zakri, J.-P. Laurent, and M. Vauclin, J. Phys. D **31**, 1589 (1998).
[81] A.V. Goncharenko, V.Z. Lozovski, and E.F. Venger, Opt. Commun. **174**, 19 (2000).
[82] A.V. Goncharenko, I.E. Khomenko, and E.F. Venger, in *Conference on Light Scattering by Nonspherical Particles: Theory, Measurements and Applications* (AMS, Providence, RI, 1998), pp. 173–176.
[83] E.F. Venger, A.V. Goncharenko, and M.L. Dmitruk, *Optics of Small Particles and Disperse Media* (Naukova Dumka, Kyiv, 1999).
[84] E.F. Venger, A.V. Goncharenko, N.L. Dmitruk, and V.R. Romaniuk, Opt. Spectrosc. **84**, 232 (1998).
[85] A.V. Goncharenko, E.F. Venger, and S.N. Zavadskii, J. Opt. Soc. Am. B **13**, 2392 (1996).
[86] A.V. Goncharenko, Yu.G. Semenov, and E.F. Venger, J. Opt. Soc. Am. A **16**, 517 (1999).
[87] H. Scher and R. Zallen, J. Chem. Phys. **53**, 3759 (1970).
[88] R. Zallen, *The Physics of Amorphous Solids* (Wiley, New York, 1983).
[89] D. Stauffer, *Introduction to Percolation Theory* (Taylor and Francis, London, 1985).
[90] *Fractals and Disordered Systems*, 2nd ed., edited by A. Bunde and S. Havlin (Springer-Verlag, Heidelberg, 1996).
[91] I. Balberg, C.H. Anderson, S. Alexander, and N. Wagner, Phys. Rev. B **30**, 3933 (1984).
[92] I. Balberg, Phys. Rev. B **31**, 4053 (1985).
[93] I. Balberg, Philos. Mag. B **56**, 991 (1987).
[94] A. Drory, I. Balberg, U. Alon, and B. Berkowitz, Phys. Rev. A **43**, 6604 (1991).
[95] A. Drory, Phys. Rev. E **54**, 5992 (1996).
[96] A. Drory, Phys. Rev. E **54**, 6003 (1996).
[97] A. Drory, B. Berkowitz, G. Parisi, and I. Balberg, Phys. Rev. E **56**, 1379 (1997).
[98] The Potts fluid is defined as a system of interacting s-state spins which are free to move in the continuum. In its turn, a pair-spin interaction is defined via the probability of disconnection.
[99] W. Xia and M.F. Thorpe, Phys. Rev. A **38**, 2650 (1988).
[100] E.J. Garboczi, M.F. Thorpe, M.F. DeVries, and A.R. Day,

Phys. Rev. A **43**, 6473 (1991).
[101] E.J. Garboczi, K.A. Snyder, J.F. Douglas, and M.F. Thorpe, Phys. Rev. E **52**, 819 (1995).
[102] E.J. Garboczi, Annu. Rev. Comput. Phys. **7**, 85 (2000).
[103] J.N. Roberts and L.M. Schwartz, Phys. Rev. B **31**, 5990 (1985).
[104] K.R. Mecke and A. Seyfried, Europhys. Lett. **58**, 28 (2002).
[105] R.F. Voss, R.B. Laibowitz, and E. Allessandrini, Phys. Rev. Lett. **49**, 1441 (1982).
[106] S. Blacher, F. Brouers, P. Gadenne, and J. Lafait, J. Appl. Phys. **74**, 207 (1993).
[107] E. Dobierzewska-Mozrzymas, P. Bieganski, and J. Wojcik, Vacuum **48**, 293 (1997).
[108] K. Seal, M.A. Nelson, Z.C. Ying, D.A. Genov, A.K. Sarychev, and V.M. Shalaev, Phys. Rev. B **67**, 035318 (2003).
[109] B. Abeles, H.L. Pinch, and J.I. Gittleman, Phys. Rev. Lett. **35**, 247 (1975).
[110] S. Barzilai, Y. Goldstein, I. Balberg, and J.S. Helman, Phys. Rev. B **23**, 1809 (1981).
[111] G.A. Niklasson and C.G. Granqvist, J. Appl. Phys. **55**, 3382 (1984).
[112] T.W. Noh, Y. Song, S.-I. Lee, J.R. Gaines, H.D. Park, and E.R. Kreidler, Phys. Rev. B **33**, 3793 (1986).
[113] Y. Song, T.W. Noh, S.-I. Lee, and J.R. Gaines, Phys. Rev. B **33**, 904 (1986).
[114] A. Mammou, A. Brau, A. Azema, J.-P. Farges, and A. Gilabert, Physica C **233**, 349 (1994).
[115] C.C. Chen and Y.C. Chou, Phys. Rev. Lett. **54**, 2529 (1985).
[116] I.G. Chen and W.B. Johnson, J. Mater. Sci. **26**, 1565 (1991).
[117] J. Wu and D.S. McLachlan, Phys. Rev. B **56**, 1236 (1997).
[118] D.S. McLachlan, J. Electroceram. **5**, 93 (2000).
[119] J.A. Sherwin, A. Lakhtakia, and B. Michel, Opt. Commun. **178**, 267 (2000).
[120] Generally speaking, even for 3D hard (nonoverlapping) identical particles the higher bound of the percolation threshold can exceed 1/2. Obviously, it corresponds to close packing of the particles. It is of interest that even for particles of the simplest (spherical) shape there is no consensus on what is the *random* close packing value [see, e.g., S. Torquato, T.M. Truskett, and P.G. Debenedetti, Phys. Rev. Lett. **84**, 2064 (2000)]. As for ellipsoidal particles, they can form packing with a degree of orientational order [see B.J. Buchalter and R.M. Bradley, Europhys. Lett. **26**, 159 (1994)]. This fact obviously complicates determining the percolation threshold higher bound.
[121] Q. Xue, Physica B **325**, 195 (2003).
[122] W. Lamb, D.M. Wood, and N.W. Ashcroft, Phys. Rev. B **21**, 2248 (1980).
[123] R. Hilfer, Adv. Chem. Phys. **92**, 299 (1996).
[124] J. Sturm, P. Grosse, and W. Theiss, Z. Phys. B: Condens. Matter **83**, 361 (1991).
[125] A.R. Day and M.F. Thorpe, J. Phys.: Condens. Matter **11**, 2551 (1999).
[126] A.R. Day, A.R. Grant, A.J. Sievers, and M.F. Thorpe, Phys. Rev. Lett. **84**, 1978 (2000).
[127] W. Theiss, Adv. Solid State Phys. **33**, 149 (1993).
[128] E. Gorges, P. Grosse, J. Sturm, and W. Theiss, Z. Phys. B: Condens. Matter **94**, 223 (1994).
[129] See, e.g., C. Brosseau, A. Beroual, and A. Boudida, J. Appl. Phys. **88**, 7278 (2000), and references therein.
[130] A. Dotsenko, S.A. Kuchinsky, and M. Prassas, J. Non-Cryst. Solids **218**, 317 (1997).